EXPERIMENTAL EVALUATION OF VEHICLE CABIN NOISE USING SUBJECTIVE AND OBJECTIVE PSYCHOACOUSTIC ANALYSIS TECHNIQUES

Nebojsa Radic[1], Colin Novak[2], and Helen Ule[2]
[1]ABC Air Management Systems Inc., 51 Rexdale Blvd., Toronto, Ontario, Canada, M9W 1P1
[2]Dept. of Mechanical Engineering, University of Windsor, 401 Sunset, Ontario, Canada, N9B 3P4 novak1@uwindsor.ca

ABSTRACT

Given the automotive industry's awareness of the importance of the perception of noise, vibration and harshness (NVH) emissions, there is an increased focus on the sound quality of automotive vehicle cabin noise. Psychoacoustic analysis using acoustic pressure measurements taken inside the vehicle cabin was performed. Suspension vibration measurements from several structural positions were also taken to evaluate vibration excitations. The goal was to be able to predict the psychoacoustic impact at the driver's ear position using the suspension vibration data measured outside the vehicle. Using the vibration data, it was possible to evaluate the transfer path of the excitation energy into the vehicle cabin. Using this, a correlation between the predicted in-cabin psychoacoustic results using the outside vibration measurement data and the direct psychoacoustic calculations from the in-cabin noise measurements was proven possible with some inherent limitations.

SOMMAIRE

Compte tenu de la reconnaissance par l'industrie d'automobile de l'importance de la perception des émissions de NVH, il y a maintenant plus de concentration sur la qualité sonore du bruit à l'intérieur des automobiles. L'analyse psycho-acoustique a été effectue avec l'aide des mesures des pressions acoustiques à l'intérieur du véhicule. Les mesures des vibrations de la suspension de l'automobile ont été prises à plusieurs positions structurelles pour évaluer les excitations de vibration. En utilisant les données de bruit et de vibrations, il a été possible d'évaluer le moyen de transfert de l'énergie d'excitation de la suspension à l'intérieur du véhicule. Une tentative d'établir une corrélation entre les mesures de bruit et de vibrations et les observations psycho-acoustiques a été possible avec certaines limites.

INTRODUCTION

In terms of noise generation, the automobile is simply a set of different systems that when excited at specific frequencies will eventually lead to the creation of noise. This statement was of course also true in the early days of automobiles, however, it was always taken to be a secondary issue that was simply accepted since more important factors had to be addressed. Both technology improvements and legislative advancements have since led to the evolution of the modern automobiles and the development of new performance targets, some of which target noise.

Today, automakers invest significant time and money in research and development associated with the reduction of vehicle noise. Since automakers are also more aware of the importance of the perception of noise, vibration and harshness (NVH) emissions, there is also an increased focus on the sound quality of vehicle cabin noise. Consumers also demand safer and more comfortable vehicles, especially given the significant increased use of cellular phones, entertainment and interactive voice controls in vehicles. As part of this, the evaluation of vehicle cabin acoustics using psychoacoustic metrics has become an essential tool for the improvement of today's vehicles. It would be very useful if these psychoacoustic impacts at the driver's ear position could be determined indirectly by using noise or vibration measurement data taken at the source location, usually outside of the vehicle or under the hood. This would result in saving of time and money by being able to use existing measurement data, often supplied by tier one and two suppliers, without the need to collect additional binaural noise data using a vehicle chassis dynamometer for specific psychoacoustic post processing.

A significant source of unwanted cabin noise is the result of external sources such as engine components, drivetrain and road-induced excitation of the vehicle suspension all of which propagate into the vehicle cabin. [1] [2]. The purpose of this study is to investigate whether vehicle suspension noise and vibration data could be used to predict the sound quality metrics of loudness, fluctuation strength and roughness as well as sound pressure level at the driver's ear position. Specifically, an evaluation of the transmission paths of the excitation energy into the vehicle cabin from road induced noise and vibration using frequency response functions is performed. As part of this, binaural noise data was also taken in the vehicle and post processed to calculate the same sound quality metrics. The objective is to establish a correlation between the suspension measurements taken outside of the vehicle to the

psychoacoustic calculation results based on measured noise data taken inside the vehicle at the driver's ear position.

THEORY OF PSYCHOACOUSTIC METRICS

The study of psychoacoustics involves the quantification of the human perception of sound [3]. In other words, it aims to correlate physical acoustic parameters to actual sound perception. There are many different psychoacoustic metrics that are used today. The ones considered in this study include Zwicker Loudness, Roughness and Fluctuation Strength. A description of each follows.

Zwicker Loudness - To understand the metric of Zwicker loudness, an understanding of frequency sensitivity and masking is also necessary. For this, the following parameters need also to be considered:

- Frequency and sound pressure level (SPL) level influence
- Critical Bands and
- Frequency Masking

Sound is not perceived equally across the entire frequency range. The human ear is most sensitive at frequency within the approximate range of 2.5 kHz to 5 kHz. Further from 4 kHz in either direction, sensitivity of human hearing decreases. In order to characterize these differences, equal loudness curves (Figure 1) have been developed and evolved over the years. The latest version of these curves have been standardized by ISO 226:2003 [4] and illustrate the human sensitivity of sounds at different sound pressure levels as a function of frequency. Loudness unity is taken to be at a 1 kHz pure tone having an SPL of 40 dB and is given as 1 sone. This reference value is also often expressed as a loudness level having a value of 40 phons. However, the expression of this metric using the units of sones has the advantage that the loudness can be expressed in a linear manner. In other words for a given a noise source which is increased to be twice as loud, the perceived loudness value is also doubled.

It is common practice that the frequency content of a signal be given in terms of full or fractional octave bands. The human hearing system instead filters sound with respect to frequency using bandwidths referred to as "Critical Bands" for which there are 24 bands in total [5][6].

It has also been shown that masking of a sound can occur for sounds which are present within adjacent bands. This phenomenon of frequency masking, which is accounted for in the calculation of Zwicker loudness, can occur when two nearby coexist as illustrated in Figure 2. Here, the dashed curve represents the masking pattern of the masker tone. The term "frequency masking" comes from the fact that if two signals are present in the same or nearby frequency band, the stronger signal will overshadow the weaker signal. Heard separately, one is able to clearly distinguish between them, however, once they occur simultaneously, the sound with the lower SPL level will be less audible or in the case where the masked tone is below the masking pattern, it will not heard at all. It should also be noted that as a masker tone becomes louder, the right side of the masking pattern slope becomes flatter and results in a greater ability to mask sounds having frequencies further away from the frequency of the masker tone. This effect is called the "non-linear upward spread of masking". [7]

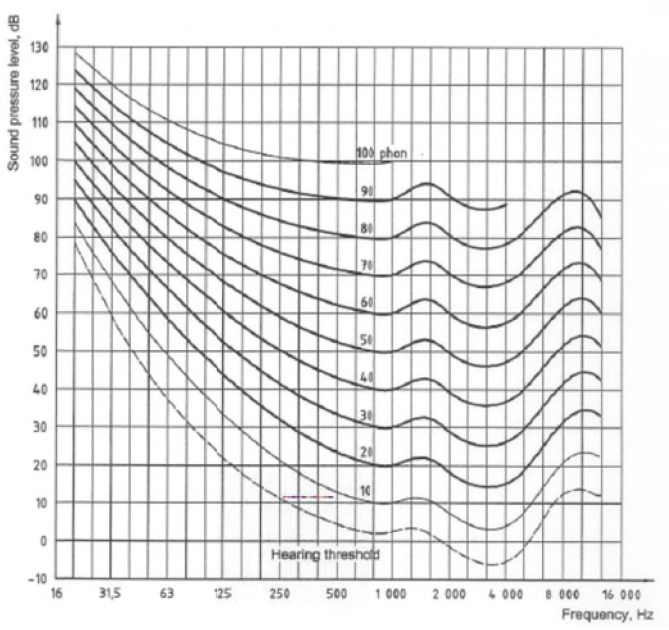

Figure 1: *Equal Loudness Curves* [4]

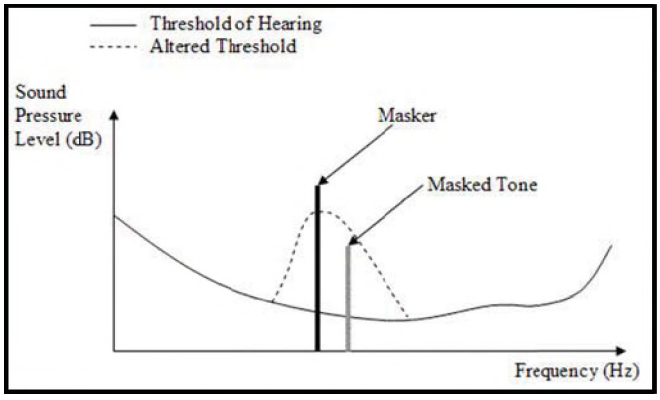

Figure 2: *Frequency Masking* [8]

Examination of the necessary derivations given by Fastl and Zwicker [9] including "specific loudness" (N') begins with the assumption that a relative change in intensity or excitation level (E) is proportional to a relative change in perceived loudness. We have:

$$\frac{\Delta N'}{N'} = k\frac{\Delta E}{E} \tag{1}$$

where: k represents the proportionality constant

Zwicker and Fastl gave an approximation for the specific loudness for each critical band as:

$$N' = 0.08\left(\frac{E_{TQ}}{E_O}\right)^{0.23}\left(\left(0.5+\frac{E}{2E_{TQ}}\right)^{0.23}-1\right)\frac{sone}{Bark} \tag{2}$$

where: E_{TQ} represents the excitation level at threshold of quiet and E_{TQ} is the excitation level at reference intensity of $10^{12}\left(W/m^2\right)$ and each having units of decibel.

The total loudness (N) can be found as the sum of specific loudness N' across all of the critical bands with critical band width (dz).

$$N = \int_0^{24Bark} N'dz \tag{3}$$

Modulating Metrics - Modulating sounds within a specific frequency range can produce two different hearing sensations. In the case of low frequency modulation (below 20 Hz) fluctuation strength is the relevant metric. For the frequency range between 20-300 Hz, the modulation may be described using Roughness. Both of these metrics are modeled in a similar manner (Figure 3) and show proportionality with respect to both modulation frequency (f_{mod}) and temporal masking depth (ΔL) [10].

$$F.S. \sim \frac{\Delta L}{\frac{f_{\mathrm{mod}}}{4Hz}+\frac{4Hz}{f_{\mathrm{mod}}}} \tag{4}$$

and

$$R \sim \Delta L * f_{\mathrm{mod}} \tag{5}$$

Modulated sounds for modulation frequencies below 20 Hz are characterized using Fluctuation Strength which is strongly dependent on the modulation frequency (f_{mod}) and temporal masking depth (ΔL). A modulation frequency of 4 Hz is found to be perceived as most annoying. [11] The temporal masking depth (ΔL) according to Zwicker and Fastl model can be approximated using both maximum ($N'_{\max}$) and minimum ($N'_{\min}$) values of specific loudness for each critical band. The term dB/Bark is simply a unit conversion.

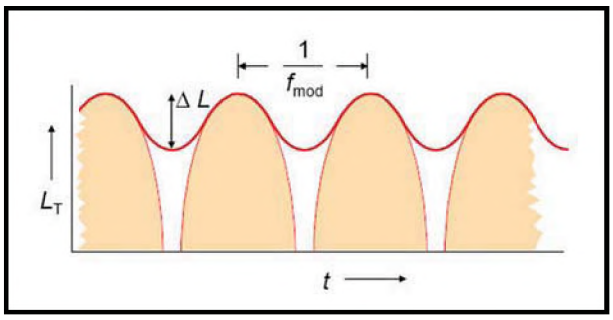

Figure 3: *Model for "fluctuation strength" & "roughness"* [10]

$$\Delta L \approx 4\log\left(N'_{\max}/N'_{\min}\right) \tag{6}$$

Substituting Eq. 3.7 into Eq. 3.5 fluctuation strength can be found to be:

$$F.S. = \frac{0.008 * \int_0^{24Bark} \frac{4\log\left(N'_{\max}/N'_{\min}\right)dB}{dB/Bark}dz}{\frac{f_{\mathrm{mod}}}{4Hz}+\frac{4Hz}{f_{\mathrm{mod}}}} \tag{7}$$

Even though the model shown in Figure 3 illustrates both fluctuation strength and roughness, the sensation of roughness when compared to fluctuation strength is actually quite different. The main difference with Roughness from a subjective perspective is the rapid amplitude modulation in the frequency range between 20 and 300 Hz. Temporal masking depth (ΔL) depends on the critical band rate, so continuing from Equation 5, a more accurate proportionality is:

$$R \sim f_{\mathrm{mod}} \int_0^{24Bark} \Delta L(z)dz \tag{8}$$

Finally, according to Zwicker and Fastl Roughness is calculated as:

$$R \sim 0.3\frac{f_{\mathrm{mod}}}{1kHz}\int_0^{24Bark}\frac{20\log\left(N'_{\max}/N'_{\min}\right)dB}{dB/Bark}dz \tag{9}$$

Frequency Response Functions & Coherence - When considering dual signal analysis, the frequency response function (FRF) is a particularly valuable tool. It is used to represent the relationship between the input and the output signal of the system upon the transformation of data from the time to frequency domain. Figure 4 illustrates an overview of the required steps for the estimation of FRFs. There are four main stages: recording, analysis, averaging, and post-processing.

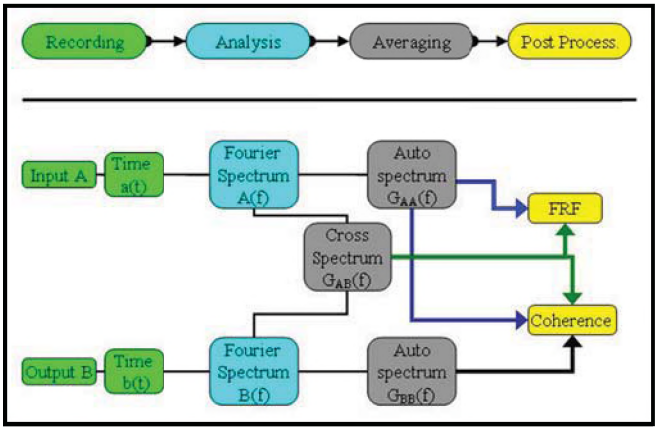

Figure 4: *Schematic representation of dual signal analysis*

The recorded time signal is transformed to the frequency domain via the FFT process. Auto-spectrums of both input and output signal individually as well as the cross-spectrum between them are obtained through the process of averaging. This finally leads to the derivation of the frequency response function and coherence.

The Fourier spectrum of the signal a(t) and b(t) is given as A(f) and B(f) respectively and can be found as:

$$A(f) = \int_{-\infty}^{\infty} a(t) e^{-j2\pi ft}\, dt \tag{10}$$

This quantity is complex containing both modulus and phase. In order to find the auto-spectrum, G_{AA} (i.e. G_{BB}), Fourier spectrum $A(f)$ (i.e. $B(f)$), is multiplied by its complex conjugate and averaged. This will produce a real and positive number because of the complex squaring.

$$G_{AA} = \overline{A^*(f) * A(f)} \tag{11}$$

Similarly, the cross-spectrum G_{AB} is defined as:

$$G_{AB} = \overline{A^*(f) * B(f)} \tag{12}$$

Because of the fact that this term is complex, it contains the phase between the output and the input of the system.

Once we have all three fundamental spectra (G_{AA}, G_{BB} and G_{AB}), the frequency response function can be found as:

$$H_1(f) = \frac{G_{AB}}{G_{AA}} \tag{13}$$

Finally, to show the degree of linearity between the two signals in the frequency domain, and to validate frequency response function, the Coherence function is used. It can be calculated in the following way:

$$\gamma^2(f) = \frac{|G_{AB}|^2}{G_{AA} * G_{BB}} \tag{14}$$

where: $0 \le \gamma^2(f) \le 1$

Coherence can range from zero to one such that if equal to one at given frequency, the system has perfect causality at that specific frequency and that the output is simply caused entirely by the input. On the other hand, if the coherence is equal to zero, the output is caused entirely by another uncorrelated source. For the case of low levels of coherence, this may be caused by some extraneous noise at either the input or the output of the system or that the some other non-correlated input may be passing through the system [12]. Coherence is often used along with the frequency response function for validation and in to show the degree of linearity between an input and output signal in the frequency domain.

EXPERIMENTAL DETAILS

For this investigation, acoustic pressure measurements were taken inside the vehicle cabin at the driver's left ear location using conventional microphones as well as at the passenger's ears position with a binaural head for the evaluation of the resulting sound quality. The acquisition recording time was 15 seconds per run performed in a hemi-anechoic chamber with the vehicle driven and motored on a 4-wheel-drive dynamometer.

The vehicle used for the experiments was a 2004 Chevrolet Epica Notchback LS. The Epica is a front wheel drive vehicle powered by an inline six-cylinder engine mounted transversely. The overall body dimensions are given in Figure 5.

To prevent acoustic rattling, loose and body parts were removed and secured as shown in Figure 6. The vehicle's airbags were also removed during the tests for safety reasons and is illustrated in Figure 7.

In order to mount and secure the accelerometers on the suspension points, brackets were made and installed at the measurement positions. Aluminum brackets were machined

and bolted on the top of the McPherson strut and next to the wheel hub both on the driver's side of the vehicle as shown in the Figure 8 below.

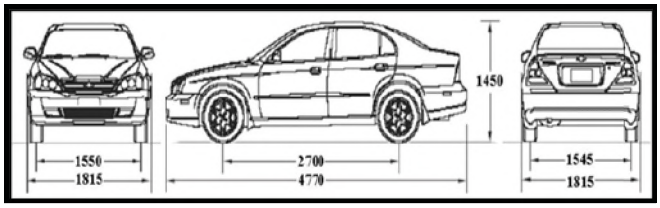

Figure 5: *Epica LS Dimensions in mm* [13]

Figure 6: *(Left) original rear end; (Right) modified rear end*

Figure 7: *(Left) original Epica's interior; (Right) modified interior-airbag removed*

Figure 8: *(Left) top of the McPherson strut; (Center) bracket next to wheel hub; (Right) lower A- arm*

An accelerometer was also attached to the suspension link on a flat portion on the bottom of the lower arm. All of the brackets were installed with the vehicle maintained at the normal riding height. They were also specifically oriented such that the accelerometer's positive x-direction was facing front of the car, the positive z-direction was facing the top of the car and the positive y-direction was oriented toward the left side of the vehicle. Microphones were located inside the vehicle cabin as well as outside of the car near the front driver side wheel. There were a total of four microphones used in the experiment. One microphone was mounted at the left side of driver's headrest (Figure 9 - *middle*) while the second was installed on the outside of the cabin next to front wheel on the driver's side (Figure 9 - *right*). For this case, a microphone windscreen was used to protect the diaphragm and reduce any wind noise effects. The other two microphones were located inside the binaural head which was installed at the passenger's seat position (Figure 9 - *left*). The head assembly was placed on a stand so as to resemble the ride height of a typical person positioned in the seat.

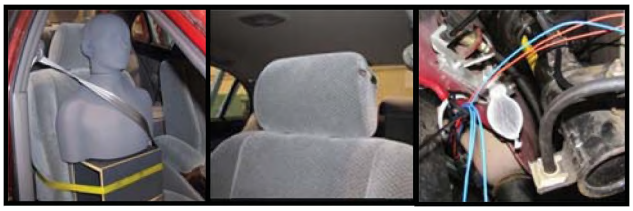

Figure 9: *(Left) passenger's seat with binaural head; (Middle) driver's seat with conventional microphone; (Right) microphone next to the front wheel*

The testing was done at the Brüel & Kjær Application Research Center (ARC) in Canton, Michigan, USA within a semi-anechoic room equipped with a 4WD dynamometer as illustrated in Figure 10.

Figure 10: *4WD dynamometer ARC anechoic chamber*

The function of the chassis dynamometer was to replicate the rolling resistance that the vehicle would experience while driven on the road. In order to ensure accurate sound measurement with minimal background noise, testing was done in a hemi-anechoic room where only the floor was reflective. The walls were treated with sound absorbing wedges thus minimizing both ambient noise and reflections and providing a room cut-off frequency of approximately 90 Hz. The dynamometer rollers had a road surface imprint adhered to them to better replicate a real driving surface taken from a local proving ground test track. For cases of self-driven and motored vehicle, the testing speed, engine load, air circulation and exhausts emissions were controlled remotely from the controlling room located next to the test cell. Data acquisition was performed during motored and driven conditions. For both cases, the following operation conditions were considered:

- Idling/Ambient
- Steady speeds (20, 40, 50, 60 & 80 km/hr)

- Acceleration run-up from 0 to 80 km/hr

For the vibration acquisition, the accelerometer positioned on the wheel hub and was stationary for the entire experiment. The second accelerometer was moved between tests, initially located on the lower A-arm it was later moved to the top of the McPherson strut. Because of the effect of heat generation by the brake calliper, a piezoelectric accelerometer was to used due to its heat resistant qualities. Six Brüel & Kjær Type 2635 and Type 2626 amplifiers were used to condition the two 3-axis accelerometers. For each steady speed run, 15 second data was collected, whereas for the acceleration tests, approximately 30 seconds of acquisition was required due to the maximum possible acceleration rate of the dynamometer.

DATA ANALYSIS

Two commercial software packages were used for the purpose of calculation of psychoacoustic metrics. The pure aqcuired time signals were used for the determination of the frequency response functions (FRF) and coherence between the pressure and acceleration excitations from outside of the vehicle and the sound pressure obtained inside the cabin,. Separate Matlab codes were also made to estimate pressure levels using these FRFs.

The psychoacoustic metrics of Loudness, Roughness and Fluctuation Strength as well as the A-weighted SPL at steady driving speeds were processed. For this purpose, a software program called dBSonic was used. Selected signals from all three microphones located in the vehicle cabin were considered at all steady speeds in both cases of self-driven and motored vehicle. This particular software allowed for the selection of the desired sound files and by specifying specific parameters, for example, frequency weighting for SPL, window type or window overlap for FFT spectrograms or type of sound field and interval between points for psychoacoustic metrics, the desired results can be obtained. Figure 11 shows a schematic representation of an analysis performed using dBSonic.

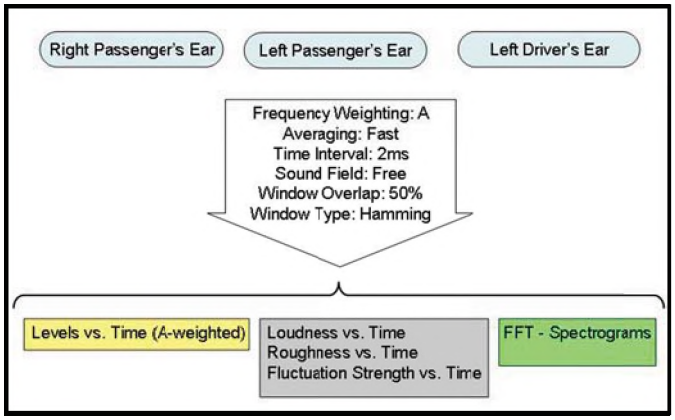

Figure 11: *Schematic representation of analysis performed using dBSonic.*

Estimation of the relationship between the input and the output of the system was performed using the two different software programs dBFA and Matlab. For this process, each of the ten input signals needed to be correlated to each of the three output signals. Two different trials were also considered at six different steady speeds. Additionally, two different driving conditions were considered which gave frequency response functions and coherence functions for correlation between the sound pressure from outside and sound pressure inside the vehicle cabin.

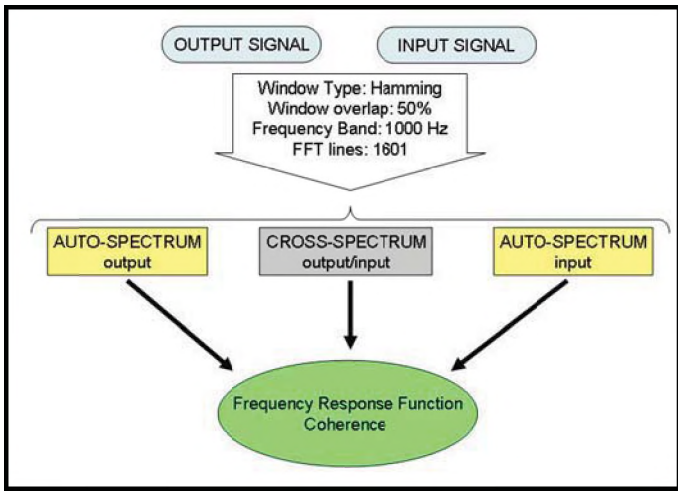

Figure 12: *Schematic representation of analysis performed using dBFA.*

For the first case, the raw signal was loaded into dBFA for post-processing. In order to generate the frequency response and coherence functions between any input and output signal a few steps must first be completed as illustrated in Figure 12. First, the two signals of interest are selected. And the auto-spectrum and cross-spectrum of each of them are found using narrow band spectrum analysis. The FFT window type was then selected as well as the window overlap and the number of FFT lines. To reduce computational time, the frequency band was specified in this case to be limited to 1000 Hz. The cross-spectrums were calculated in the same manner making sure that all of the selected parameters match the ones used for auto-spectrum calculations to be able to compute the Transfer Functions, FRFs and Coherence values.

From the Auto-spectrums G_{AA} (input) and G_{BB} (output) as well as the cross spectrum G_{AB} between the input and the output, analysis produces the transfer function:

$$H_1(f) = \frac{G_{AB}}{G_{AA}}$$

and Coherence:

$$\gamma^2(f) = \frac{|G_{AB}|^2}{G_{AA} * G_{BB}}.$$

Given that the acquisition software does not allow for the calculation of frequency response functions between pressure and/or acceleration or any of the psychoacoustic metrics, Matlab codes were developed using the basic built-in functions within Matlab for the calculation of the auto-spectrums and the cross-spectrums separately. These were then combined to calculate the FRFs and coherence using built-in functions for direct estimation of both FRFs and coherence.

The Matlab function was used to estimated the transfer function of the system with input A and output B using Welch's averaged periodogram method. Coherence is also estimated in the similar matter. They are both given as:

[Txy, F] = tfestimate (A, B, WINDOW, NOVERLAP, NFFT, Fs, 'whole')

[Cxy, F] = mscohere (A, B, WINDOW, NOVERLAP, NFFT, Fs, 'whole')

Where:

A	Input Signal (Time Domain)
B	Output Signal (Time Domain)
WINDOW	Specific Window function
NOVERLAP	Percentage of overlap between segments
NFFT	Number of FFT points
Fs	Sampling frequency
'whole' / 'half'	Whole or half of the Nyquist interval

Consider for example the case where the vehicle was self driven at the steady speed of 40 km/hr. Given that there were two trials per speed, trial #1 was used to find frequency response functions between input and output signal. The calculated FRF would be then used to estimate the output signal from the second trial. The relationship between the input and the output of the system can be represented as:

$A(f) * H_1(f) = B(f)$ where H1 is the FRF of the system.

This expression is valid in the frequency domain so once the output has been estimated, it would be given in the frequency domain. As such, the inverse of the FFT of the signal was required to obtain the signal in the time domain.

At this point, a comparison was possible between the original and predicted levels to see if the FRFs are valid as well as the resulting confidence levels (Figure 14). Also obtained were the values of sound pressure which was further analyzed by loading the sound files into dBSonic for analysis of the psychoacoustic metrics.

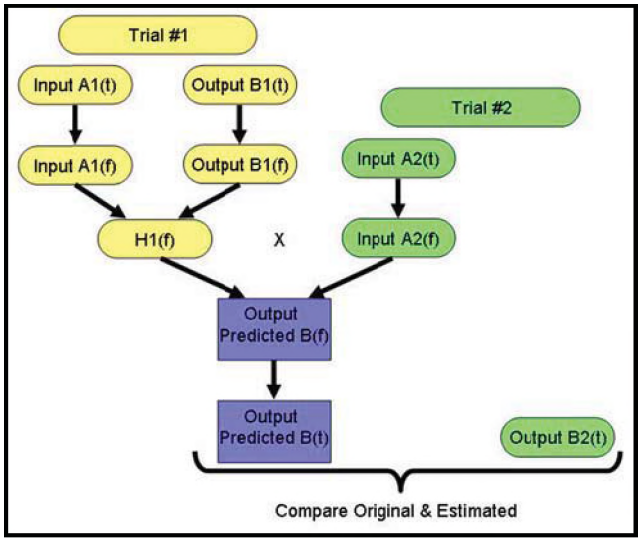

Figure 13: *Schematic representation of pressure estimation using Matlab*

RESULTS & DISCUSSIONS

The following section provides some examples of the calculated frequency response functions obtained in order to present a relationship between the system inputs and outputs as well as how they relate to each other. The ten input signals (all at front driver's side) are as follows:

1. Outside Microphone (Next to the wheel)
2. Acc #1 - Longitudinal Direction (Wheel hub)
3. Acc #1 - Lateral Direction (Wheel hub))
4. Acc #1 - Vertical Direction (Wheel hub)
5. Acc #2 - Longitudinal Direction (Lower A-arm)
6. Acc #2 - Lateral Direction (Lower A-arm)
7. Acc #2 - Vertical Direction (Lower A-arm)
8. Acc #3 – Long. Direction (Top McPherson strut)
9. Acc #3 – Lateral Direction (Top of McPherson strut)
10. Acc #3 - Vertical Direction (Top of McPherson strut)

The system consisted of three microphone outputs from inside of the vehicle:

1. Microphone #1 - Left driver's headrest
2. Microphone #2 - Left passenger's ear
3. Microphone #3 - Right passenger's ear

Testing was done at six different steady speeds. These were all performed with the conditions of the vehicle being driven

and motored. As this provided hundreds of different FRFs and coherence functions, discussions in this section will be limited to only provide few of the examples to illustrate the main points. Typical results for two microphone signals are similar to Figure 14 where the top graph represents the frequency response function and the bottom one shows the coherence function which corresponds to the degree of linearity between the two signals in the frequency domain.

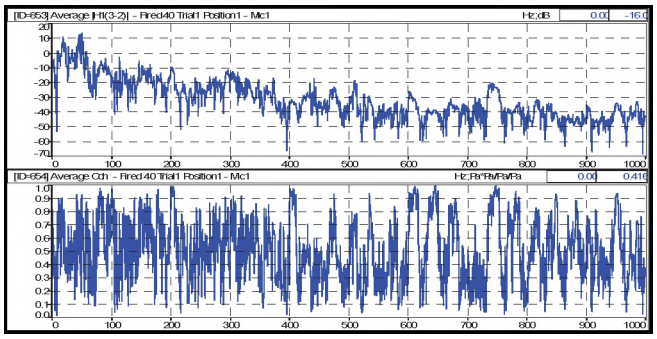

Figure 14: *Illustration of Frequency Response Function (Top) and Coherence (Bottom) between Outside Microphone and Passenger's Right Ear for Self-Driven Car at 40 km/hr*

Figure 15 illustrates the FRFs and coherence of the vibration data signal that is correlated to the pressure inside the vehicle. The blue line represents the longitudinal vibration direction, the red line the lateral and the green line represents the vertical direction of the vibration. All three directions generally follow the same trend; however, the vertical direction usually gave slightly higher results then the other two. This is the most important direction since humans are most sensitive to vibration in the vertical direction [14]. However, this cannot be taken as a general rule since at different speeds and at different accelerometer positions, variations are present. When inspecting all the different inputs, one can also see that they are all relatively comparable to each other and that only slight variations are present. It is difficult to make any kind of general statement that applies to all the different inputs as well as all the different speeds simply because there are so many of them.

In general, the coherence levels do not look particularly promising. For the case of low levels of coherence near to zero, this may be caused by some extraneous noise at either the input or the output of the system or that the some other non-correlated input may be passing through the system [12]. In general for automotive applications, vibration data with coherence levels over 70% and acoustic excitation data above 60% respectively, have been shown to be used to successfully estimate interior sound and vibration levels [14]. For this investigation, it was found that the vertical vibration data and noise data taken under the condition of steady speed on a motored dynamometer condition provided the best coherence results.

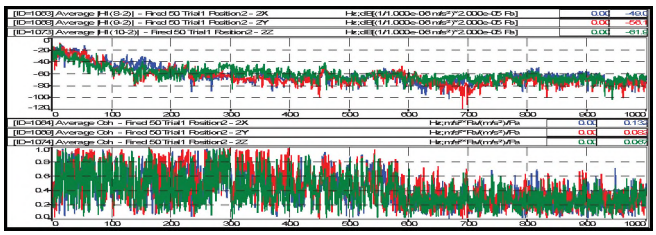

Figure 15: *Illustration of Frequency Response Functions (Top) and Coherence (Bottom) between Acc #3 (All three directions and Passenger's Right Ear for Self-Driven Car at 50 km/hr*

To verify the quality of the FRFs, especially with the poor coherence levels, one needs to look at how they can be used to predict pressure levels. Obtained frequency response functions were used to calculate and predict pressure values inside the vehicle based on one of the inputs from outside. One of the trials was used to calculate the FRF from the input and output signals and that FRF would later be applied to one of the input signals from another trial to predict a new value. If one were to look at the original and predicted levels for the case of the motored vehicle at 60 km/hr (Figures 16 & 17), one can see that the predicted pressure levels are very similar. Both microphone and accelerometer stimuli can be used to obtain pressure inside the car; however, we need to be aware that different acceleration directions can give better results when compared to others. This section was used to quickly check the validity of predicted results and not to examine all of them.

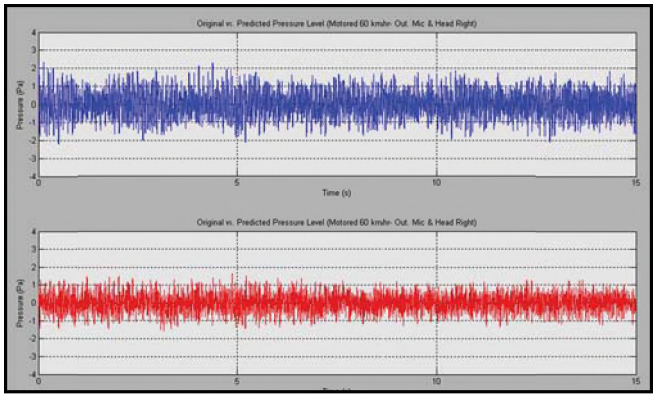

Figure 16: *Illustration of Original (Top) and Predicted (Bottom) Pressure Levels for Motored Car at 60 km/hr between Outside Microphone and Passenger's Right Ear*

One can use already predicted values of pressure obtained earlier in order to calculate the psychoacoustic metrics. The following Figures 18 to 21 show agreement between the original and calculated levels for all metrics. At this point, the 60 km/hr motored vehicle is taken arbitrary simply to illustrate this point. At this particular speed, the predicted mean levels of A-weighted sound level are within 2 dB with respect to the original data. It is commonly know that a difference of 3 dB represents the threshold of human perception of change in level. As such, the 2 dB difference represents a variation that is likely indistinguishable to

human perception. Roughness and fluctuation strength showed excellent agreement as well.

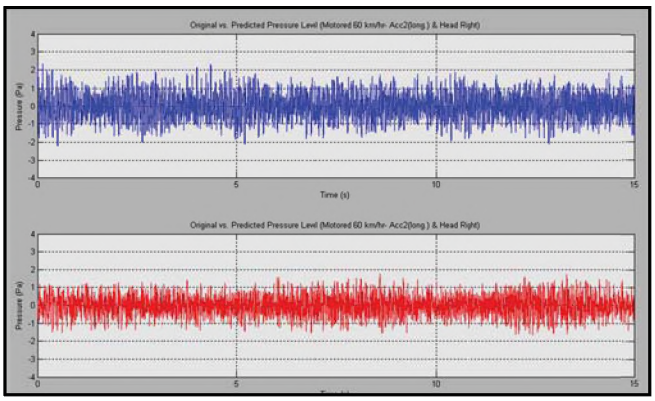

Figure 17: *Illustration of Original (Top) and Predicted (Bottom) Pressure Levels for Motored Car at 60 km/hr between Acc #2 in Longitudinal Direction and Passenger's Right Ear*

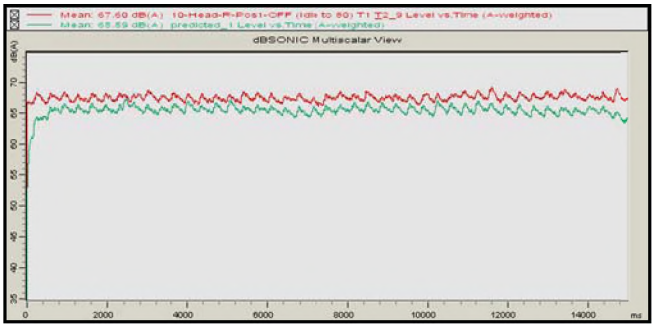

Figure 18: *Illustration of Original (Red) and Predicted (Green) A-weighted SPL for Motored Car at 60 km/hr found at Passenger's Right Ear*

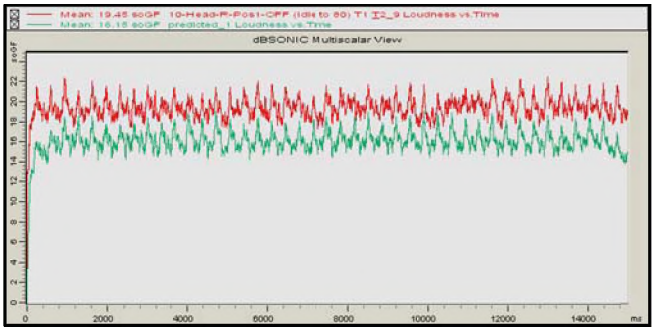

Figure 19: *Illustration of Original (Red) and Predicted (Green) Loudness for Motored Car at 60 km/hr found at Passenger's Right Ear*

CONCLUSIONS

Presently one of the major development issues for the automotive industry is automotive cabin noise. As a result, significant effort is being done to both reduce sound levels as well as improve the sound quality in order to give the consumer a more enjoyable driving environment. Having said this, it is critical to gain an understanding about the different noise sources and their relationship with the receiver points of interest.

An attempt was made to establish a correlation between the noise and vibration measurements from the outside of the vehicle to the noise and psychoacoustic calculations of the noise measured inside the vehicle. This was proven to be possible with some inherent limitations. Direct prediction of the sound quality metrics inside the vehicle from both acceleration and sound pressure observed outside of the vehicle cabin did not show compatible results to the measured data. However, it was proven possible to predict the sound pressure for which the psychoacoustic metrics could be calculated indirectly.

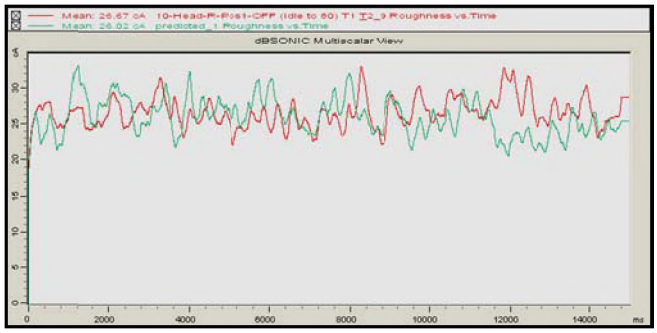

Figure 20: *Illustration of Original (Red) and Predicted (Green) Roughness for Motored Car at 60 km/hr found at Passenger's Right Ear*

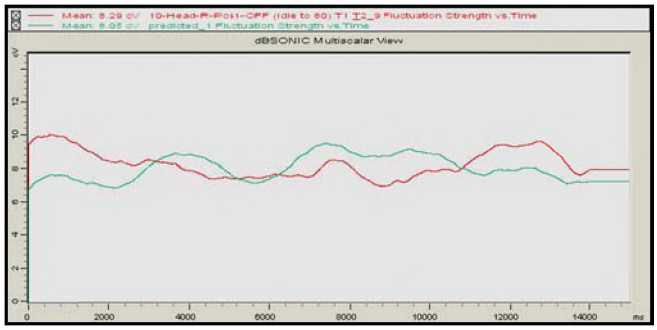

Figure 21: *Illustration of Original (Red) and Predicted (Green) Fluctuation Strength for Motored Car at 60 km/hr found at Passenger's Right Ear*

ACKNOWLEDGMENTS

The authors would like to express their gratitude for the financial support from the AUTO21 Network of Excellence.

Testing was conducted at Application Research Center (ARC) at Canton, Michigan, USA and Ford Motor Company (Windsor Engine Plant) in Windsor. The authors would like to thank the staff at both facilities for their help and expertise.

REFERENCES

1. Zavala, P., Moraes, M., Fuchs de Jesus, G., Pinheiro da Silva, S. (2006). Driveline Induced Vibration Investigation. *Society of Automotive Engineers*, 2006-01-2883.

2. Kim, M.G., et al., Reduction of road noise by the investigation of contributions of vehicle components. SAE Paper 2003-01-1718.

3. Defoe, J., Novak, C., Ule, H., Gaspar, R. (2006). A Critical Analysis of Loudness Calculation Methods. *Journal of the Canadian Acoustical Association*, p. 28, 34 (3).

4. International Organization for Standardization. ISO 226 *Acoustics - Normal Equal Loudness Contours. Standard*, Geneva: International Organization for Standardization, 2003.

5. Zwicker, E., Flottorp, G., & Stevens, S.S. (1957). Critical Band Width in Loudness Summation. Journal of the Acoustical Society of America, 29(5), 548-557.

6. Zwicker, E. (1961). Subdivision of the Audible Frequency Range into Critical Bands. Journal of the Acoustical Society of America, 33(2), 248.

7. Ule, H. (2010). Calculation of Unsteady Loudness in the Presence of Gaps through Application of the Multiple Look Theory, Windsor, Ontario: University of Windsor.

8. Cheng, E. *Analysis of Dynamic Shaping in Unaccompanied Bach*. [cited 2007 Dec 17]; Available from: http://www-scf.usc.edu/~ise575/b/projects/cheng/.

9. Fastl, H. and Zwicker, E., *Psycho-Acoustics Facts and Models*, 2007.

10. Brüel & Kjær. *Zwicker Loudness and derived Metrics*. [cited 2007 Dec 17]; Available from: http://www.otam.itu.edu.tr/e/konferanslar/Presentation/15%20Sound20%Quality%20Metrics.pdf.

11. Van Der Auweraer, H. and K. Wyckaert, Sound Quality: Perception, Analysis and Engineering. Leuven, LMS International.

12. Brüel&Kjær. *Guided Tour: Frequency Response Functions*. [cited 2007 Dec 17]; Available from: http://www.acousticeig.unige.ch/Docs/Protocoles%20Labo/Frequency%20Response%20Function%20BK.pdf.

13. Choquette, P., Optimization of Actualtor Configuration for the Reduction of Structure-Borne Noise in Automobiles. Sherbrooke, University of Sherbrook, M.A.Sc. Thesis. March 2006.

14. Kojovic, N., Vehicle Interior Sound and Vibration Numerical Estimation Method Based on Engine Radiated Sound and Mount Vibration. 2005, University of Windsor: Windsor.